Atmos. Chem. Phys. Discuss., 10, 4673–4717, 2010
www.atmos-chem-phys-discuss.net/10/4673/2010/
© Author(s) 2010. This work is distributed under
the Creative Commons Attribution 3.0 License.

Atmospheric Chemistry and Physics Discussions

This discussion paper is/has been under review for the journal Atmospheric Chemistry and Physics (ACP). Please refer to the corresponding final paper in ACP if available.

Long range transport of mercury to the Arctic and across Canada

D. Durnford, A. Dastoor, D. Figueras-Nieto, and A. Ryjkov

Air Quality Research Division, Environment Canada, 2121 TransCanada Highway, Dorval, QC, H9P 1J3, Canada

Received: 17 December 2009 – Accepted: 8 February 2010 – Published: 16 February 2010

Correspondence to: D. Durnford (dorothy.durnford@ec.gc.ca)

Published by Copernicus Publications on behalf of the European Geosciences Union.

Abstract

This study is the most extensive study to date on the transport of mercury to the Arctic. Moreover, it is the first such study to use a fully-coupled, online chemical transport model, Environment Canada's Global/Regional Atmospheric Heavy Metals model (GRAHM), where the meteorology and mercury processes are fully integrated. It is also the only study to date on the transport of mercury across Canada. We determined source attribution from Asia, North America, Russia and Europe at six arctic verification stations, as well as three subarctic and eight midlatitude Canadian stations.

We have found that Asia, despite having transport efficiencies that were almost always lower than those of North America and often lower than those of Russia, was the dominant source of gaseous atmospheric mercury at all verification stations: it contributed the most mercury (29–37% at all stations, seasons and levels considered), its concentrations frequently explained nearly 100% of the variability in the concentrations produced by the simulation performed with full global emissions, particularly in the absence of local sources, and it generated the most long range transport (LRT) events, causing 43%, 67% and 75% of the events at the arctic, subarctic and midlatitude stations, respectively. For the Arctic, Russian transport efficiencies tended to be the strongest, as expected, while European and Asian efficiencies were lower and higher, respectively, than those found in the literature. This disagreement is likely produced by mercury's long lifetime relative to that of other pollutants. The accepted springtime preference for the trans-Pacific transport of Asian pollution was evident only in the midlatitude group of stations, being masked in the arctic and subarctic groups by the occurrence of atmospheric mercury depletion events. Some neighbouring arctic stations recorded dissimilar numbers of LRT events; despite their proximity, the behaviour of mercury at these stations was governed by different dynamics and transport pathways. The column burden of GEM in the lowest 5 km of the Northern Hemisphere was largest in summer from Asia, North America and Russia, but in winter from Europe. In the vertical, transport of mercury from all source regions occurred principally

ACPD

10, 4673–4717, 2010

in the mid-troposphere.

1 Introduction

Mercury, which is non toxic, can be converted to methylated mercury, a potent neurotoxin, in the presence of bacteria. This process is known to occur in oceans (Sunderland et al., 2009), freshwater wetlands (Goulet et al., 2007) and peatlands (Mitchell et al., 2008). Consuming fish with elevated levels of methylmercury can cause severe health problems in humans (Sunderland et al., 2009).

Mercury is emitted into the atmosphere from natural deposits on land and in oceans and as a result of anthropogenic activity. Once in the atmosphere, it is advected by winds. Since the lifetime of gaseous elemental mercury (GEM) has been estimated at between 6 months and 2 years (Strode et al., 2008; Lin et al., 2006, Schroeder and Munthe, 1998), it can be transported considerable distances from its source region. Oxidation of GEM produces reactive gaseous mercury (RGM) and mercury associated with particles (PHg) (Lin et al., 2006), which only have lifetimes on the order of days (Faïn et al., 2009, Schroeder and Munthe, 1998). Deposition occurs through scavenging by precipitation, and also as a result of resistances dominated by the canopy/surface (Lin et al., 2006). Once deposited, RGM and PHg may reduce to GEM and be reemitted (Steen et al., 2009). The repetition of the deposition and reemission cycle constitutes mercury's so-called grasshopper motion (Almeida et al., 2005). Thus, mercury that is emitted in one part of the world can eventually be transported to any other location. Mercury deposition in Arctic Alaska has increased three-fold since the advent of the Industrial Revolution (Fitzgerald et al., 2005)

In this study, we model the long range transport (LRT) of mercury to multiple observation stations around the Arctic, as well as to subarctic and midlatitude stations across Canada. This investigation is a component of the International Polar Year (IPY) project, Intercontinental Atmospheric Transport of Anthropogenic Pollutants to the Arctic (INCATPA). By running our model with global emissions and with emissions from a

ACPD
10, 4673–4717, 2010

specified source region alone, we are able to determine source attribution. Previous work on the long range transport of mercury includes studies on: trans-Pacific transport (Strode et al., 2008; Radke et al., 2007; Weiss-Penzias et al., 2006, 2007; Jaffe et al., 2005); transport within the Arctic (Berg et al, 2008); over Europe (Ryaboshapko et al., 2007a,b); and in the Northern Hemisphere (Travnikov, 2005). Other relevant studies, including those by Wang et al. (2009), Shindell et al. (2008), Jiang et al. (2007), Stohl (2006), and Liang et al. (2004), investigated the long range transport of carbon monoxide and other gaseous pollutants and/or aerosols. Of the mercury studies, only the GRAHM, which participated in the Ryaboshapko et al. (2007a, b) studies, and which is used in this project, is an online, fully-coupled model, such that the meteorology and mercury processes are fully integrated. Our study is also of interest in that it represents the most extensive study to date on the transport of mercury both to the Arctic and across Canada. The study also serves as an evaluation of the model, particularly in the Arctic. Meteorological and mercury processes are highly heterogeneous. Verification at multiple sites tests all processes simultaneously. This provides a large scale view of the model's performance and aids future model development. This study focuses on the long range transport of mercury; deposition will be the focus of a forthcoming companion paper.

Background information is provided in Sect. 2. In Sect. 3, we discuss ambient mercury concentrations at individual verification stations, investigating the behaviour of source attribution. We also investigate preferred mercury transport pathways through two-dimensional fields. A Summary is presented in Sect. 4.

ACPD
10, 4673–4717, 2010

2 Methodology

2.1 Data

2.1.1 Observations

We verified our model's simulation of surface-level atmospheric mercury concentrations against observations at 17 stations (Fig. 1, Table 1). In order to highlight latitudinal variations in mercury transport, we divided the 17 stations into three groups: arctic (six stations), subarctic (three stations) and midlatitude (eight stations). The arctic stations are situated throughout the Arctic, while the subarctic and midlatitude stations are in Canada alone. The stations range in altitude from sea level to 1.1 km above sea level.

Years with as complete a dataset as possible and close to 2000 or 2005 were chosen for verification; the anthropogenic emissions used are valid in 2000 and 2005 (see Sect. 2.1.2). It would be helpful if there were a dataset of mercury observations from all our stations during a single year, as this would eliminate meteorological inter-annual variability. Given that such a dataset does not yet exist, we chose to use multiple verification stations despite the range of years; evaluating model performance at multiple locations is highly beneficial for model development as it tests whether model meteorological and chemical processes work equally well under varying conditions. Furthermore, given the multiple years used, our statistical results could be interpreted as representing an average model performance during varying meteorological conditions; different atmospheric conditions occur in different years. Note that the model performance is always compared to the year as well as the location of each set of observations. Observations at all six arctic stations are of GEM. It is a matter of debate whether the form of mercury measured by the Tekran 2537 instrument (Swartzendruber et al., 2009) at the subarctic and midlatitude stations is GEM or total gaseous mercury (TGM). This is not an important distinction for this study, as only GEM is transported over long distances. Therefore, we will arbitrarily label the mercury as TGM. Since these observations are at one particular point, while model values represent the aver-

ACPD
10, 4673–4717, 2010

age value for the entire grid cell, the observations are expected to be more variable than the observations. Therefore, a running 24-h mean is calculated for all observations.

2.1.2 Model

We used Environment Canada's Global/Regional Atmospheric Heavy Metals model (GRAHM; Dastoor et al., 2008; Dastoor and Larocque 2004). GRAHM is an Eulerian model built on top of Environment Canada's Global Environmental Multiscale (GEM) weather forecasting model (Côté et al., 1998a, b). Thus, it is a fully-coupled, online chemical transport model, where meteorological and mercury processes are fully integrated. The GEM is characterized by a semi-Lagrangian advection scheme to promote stability, and an implicit time scheme to control high frequency oscillations. We configured the model to use Interactions Soil-Biosphere-Atmosphere (ISBA) land surface processes. The radiative transfer scheme, calculated every 1.5 h, is based on Fouquart and Bonnel (1980) and Garand and Mailhot (1990). Stratiform precipitation is calculated by a Sundqvist-based scheme, while deep convective precipitation is calculated by a Kain-Fritsch scheme. Turbulent mixing of meteorological and mercury species in the boundary layer is based on prognostic turbulent kinetic energy. Cloud liquid water/ice content is a prognostic model variable. GRAHM includes all chemical and physical processes related to mercury, namely emission, advection, chemical and physical transformations, and deposition. In polar regions, Atmospheric Mercury Depletion Events (AMDE) are simulated in springtime (Dastoor et al., 2008). Simulating AMDEs involves three distinct aspects: (1) the oxidation of mercury. This process includes simulating springtime "bromine explosions" (Lehrer et al., 2004), which are periodic, localized releases of oxidizing bromine species to the atmosphere; (2) the transportation of mercury-depleted air masses; and (3) air-snow exchanges of mercury, which are complex, heterogeneous processes, and are the focus of current work. It is likely that the relative importance of these three processes varies by location. The chemistry parameterization in GRAHM includes gas-phase oxidation of mercury by ozone and halogens, and aqueous-phase reduction of mercury by agents such as sul-

ACPD
10, 4673–4717, 2010

fur and through photochemistry. Wet and dry depositions are simulated using physical parameters calculated in the meteorological component of GRAHM. Dry deposition is based on the resistance approach, following Zhang et al. (2001, 2003).

We use the global anthropogenic mercury emission fields produced by Pacyna and co-workers valid in 2000 and 2005 (see, e.g., Pacyna et al., 2006). Non-anthropogenic emission estimates involve a high degree of uncertainty (Mason, 2009; Lohman et al., 2008). Our non-anthropogenic oceanic and terrestrial emissions of GEM are based on the global mercury budget of Mason (2009). Terrestrial non-anthropogenic emissions are divided into direct natural emissions, and reemissions of previously-deposited mercury. Direct natural emissions are distributed according to the natural geological enrichment of mercury. Reemissions are allocated according to the distribution of total deposition of mercury for historic years. The ratios of non-anthropogenic to anthropogenic emissions follow those of Gbor et. al. (2007) over North America and those of Shetty et al. (2008) over East Asia. The seasonal and diurnal variations of terrestrial emissions and reemissions are parameterized as a function of leaf area index and incoming direct solar radiation, based on Shetty et al. (2008). Oceanic emissions are modulated by the sea surface temperature. The horizontal distribution of the model's total mercury emissions for the year 2000 are presented in Fig. 2. Values are shown for the year 2000 since almost half of our observations are from that year (Table 1). For the year 2000, our global anthropogenic and non-anthropogenic emissions amount to 2195 and 3308 Mg, respectively. This yields total global mercury emissions of 5503 Mg, which is in the range of uncertainty for these emissions (Mason, 2009).

We run GRAHM over a global domain using a $1^{\circ} \times 1^{\circ}$ horizontal resolution and a 30-min timestep. In order to match the operational model's vertical resolution, we use 28 vertical levels from the surface to 10 hPa until November 2006 and 58 levels thereafter. We reinitialize the GRAHM every 48 h using Canadian Meteorological Centre operational analyses, and produce a series of overlapping 60-h forecasts. The first 12 hours of each 60-h forecast constitute a spinup period for the meteorology; the following 48 h simulate mercury processes. At least 3 years of successive forecasts

are produced prior to the anthropogenic emissions' year of validity; this spins up the mercury concentrations, ensuring a stable background load of mercury throughout the global atmosphere. Given significant uncertainties in emissions (Pacyna et al., 2006; Gbor et al., 2007; Shetty et al., 2008), and in mercury-related chemical processes (Lin et al., 2006), modeling the transport of mercury is a challenging task. GRAHM has been seen to perform well in past studies (Dastoor et al., 2008; Ryaboshapko et al., 2007a, b)

A 12-h running mean is calculated for the model values. This smoothing enables us to pick out important features and trends. The degree of smoothing applied to the model values is less than that applied to the observations, in consideration of the fact that model values represent the average value for the entire grid cell, while observations are point values.

For this study, we performed five simulations with GRAHM: with full global emissions (hereafter referred to as the base run) and with emissions from only Asia, North America, Russia or Europe. This enables us to determine source attribution for mercury at a given site. The locations of the four source regions, along with the division of the total emissions into anthropogenic and non-anthropogenic components, are presented in Fig. 2. Our four source regions account for 46% of global emissions; Asian emissions alone account for 30% of the total. In Asia and Europe, anthropogenic emissions exceed non-anthropogenic emissions. The reverse is true in North America, Russia and the remainder of the globe. India, which is the focus of a separate ongoing study, is not included in the Asian source region; preliminary results indicate that, although India is a major source of mercury, the dynamics acting on mercury from this region yield low transport efficiencies in the Arctic and Canada.

ACPD
10, 4673–4717, 2010

2.2 Calculations

2.2.1 Statistics

The percent contribution of a source region's mercury to the base run's concentrations is calculated using Eq. (1):

$$\text{PercentContribution} = 100 \cdot \frac{\sum_{\text{period}} \text{TGM}_{\text{source}}}{\sum_{\text{period}} \text{TGM}_{\text{base}}} \quad (1)$$

where *period* represents the time period involved, and *source* and *base* represent the run using emissions from the specified source region only and the base run, respectively.

The correlation squared is calculated following the standard method. We correlate the base run's GEM/TGM values at a given atmospheric level to the source run's values at the same level. The correlation squared indicates the degree to which a source region's mercury determines the variability in the base run's concentrations.

The transport efficiency is calculated by dividing the mean concentration produced by a source region at a given site by that region's total annual mercury emissions. Since the calculation involves total annual emissions, seasonal variations in the transport efficiency reflect the seasonality of wind and precipitation fields. The transport efficiency is helpful for policy makers, as reducing emissions from source regions with large transport efficiencies will have the greatest impact at receptor sites.

2.2.2 Long range transport events

Long range transport is defined in this study as intercontinental transport. Therefore, Russian mercury transport events at Amderma, European events at Andoya and North American events at Canadian midlatitude and subarctic stations do not qualify as LRT

events. However, North American events at Alert and European events at Ny-Ålesund do qualify as LRT events, since both stations are far from the emission sources.

The calculation of an LRT event is completely objective. At a given station, the base run's surface-level atmospheric concentrations are searched for local maxima. To be a candidate as an LRT event, a maximum must last for no more than six days and have a magnitude of at least 0.25 of the base run's standard deviation, calculated from all stations' data; using a common standard deviation ensures a constant minimum LRT event strength at all sites. Successive local maxima must be separated by at least 12 h. The given station's concentrations from each source region are then scanned for local maxima that occur within three days of the base run's maximum. The three-day window is permitted, as concentrations from a first source region may be declining at the onset of a second source region's LRT event; the LRT event is disguised until the 1st region's concentrations stabilize. A source region's local maximum must last for no more than six days and have a magnitude of at least 1.5 of the source region's standard deviation, calculated from all stations' data. The relative magnitude of the base run's maximum is permitted to be smaller than that of the source region's maximum, in view of the fact that the source region contributes only a fraction of the base run's concentration. North America's calculated standard deviation was halved, in consideration of the multitude of verification stations with local North American sources, which increase the standard deviation. Without this halving, it becomes much less likely that North American LRT events at arctic stations will be identified. If no more than two source regions exhibit local maxima collocated with the base run's maximum, they are considered LRT events. We permit two source regions to have simultaneous LRT events, as it's quite possible, for instance, that Asian mercury is transported to North America, and that subsequently Asian and North American mercury are transported together to a verification station. If more than two source regions exhibit local maxima collocated with the base run's maximum, it is considered that local dynamics are responsible for these maxima and that no LRT event has occurred.

ACPD
10, 4673–4717, 2010

3 Results

3.1 Individual stations

3.1.1 Time series of surface-level GEM/TGM

The springtime period, including AMDEs, where GEM concentrations decrease dramatically (Steffen et al., 2005), is well reproduced by the base run at all six arctic stations (Fig. 3a–f). (The seasons are defined as follows: spring is March–May, summer June–August, autumn September to November, and winter December to February.) The base run is also successful at capturing background GEM concentrations at these stations, apart from at Alert during January and February. Note that extended periods of missing data at stations experiencing AMDEs can significantly affect the calculated observed mean. This is demonstrated at Barrow, where a subjective examination indicates that the base run's and observed time series agree much more closely than the means, given in the panel title, would suggest. The observed mean is artificially depressed since observations at Barrow extend only from mid-January to mid-June; the very low springtime concentrations are included in the observed mean, but not the higher background concentrations of the rest of the year. The mean model GEM value over the six arctic stations is 1.50 ng (standard m)$^{-3}$, hereafter ng m^{-3}, while the average observed mean is 1.55 ng m^{-3} at all arctic stations excluding Barrow and Station Nord. These two stations are excluded since they have extended periods with no data. Since concentrations at Andoya and Amderma are missing mainly during non-AMDE periods, the observed mean for the four Arctic stations would likely be increased if these data were included. The highest mean is at Andoya, which is not only fairly close to European emission sources but which also experiences weaker AMDEs (Berg et al., 2008); its mean is depressed less by these events. Non-AMDE variability in the base run and observations tends to match well, particularly at Ny-Ålesund, Andoya and Amderma, which are the three stations most affected by European emissions.

Asian GEM concentrations, which range from 0.4–0.6 ng m^{-3}, are consistently con-

ACPD
10, 4673–4717, 2010

siderably higher at the six arctic stations than those of the other three source regions, which are typically on the order of 0.1–0.2 ng m^{-3}. Asian concentrations exhibit a summertime maximum. This maximum is strong at Barrow, Alert and Station Nord, weaker at Ny-Ålesund and Amderma, and absent at Andoya. North America and Russia produce noticeable summertime maxima at Barrow, while only North America produces such a maximum at Alert. The proximity of Andoya to European emission sources yields elevated European concentrations of up to 0.4 ng m^{-3}. Transport from Europe is so powerful at Andoya that the variability induced by the transport is able to mask any variability in the base run induced by springtime AMDE dynamics. The admirable reproduction by the base run of the springtime observations confirms the importance of the European emissions at this station.

Mean model base run concentrations at the three subarctic stations are higher than at the arctic stations (Fig. 3g–i). The average model value at the subarctic stations is 1.67 ng m^{-3}. This higher average reflects both the absence of AMDEs at two of the three subarctic stations, and also the mainly zonal nature of the transport of mercury emitted in the Northern Hemisphere, particularly in Asia (Fig. 7). The base run performs well at Kuujjuarapik, apart from its exaggeration of AMDE maxima and its lack of summertime variability. The problematic AMDE maxima reveal a weakness in the model's scheme to transfer mercury from the cryosphere to the atmosphere in the Hudson Bay area. As mentioned in Sect. 2.1.2, the complex, heterogeneous atmosphere/cryosphere mercury exchanges are currently an active area of research. The strong observed summertime variability at Kuujjuarapik is likely related to Kuujjuarapik's proximity to Hudson Bay; the model's lack of variability may be related to boundary layer chemistry and/or meteorological processes. The base run also fails to reproduce the summer/autumn decrease in concentrations observed at Little Fox Lake and Fort Chipewyan. However, the base run's performance in reproducing the variability in March and April at Fort Chipewyan is impressive. Excluding Fort Chipewyan, for which a substantial period of data is missing, the average of the observed concentrations at the subarctic stations is 1.55 ng m^{-3}. The inability of the model to capture

ACPD
10, 4673–4717, 2010

the summer/autumn minimum at two of these three stations produces a model station group average higher than observed.

The model shows that Asian concentrations are higher at the subarctic stations, with background values ranging from 0.4 to 0.8 ng m^{-3}., than at the arctic stations. Summertime maxima are exhibited at all three subarctic stations. North American values have also increased by approximately 0.05 ng m^{-3} from the arctic stations to a mean of ≈0.2 ng m^{-3} at the subarctic stations. Typical Russian and European values have decreased marginally. Russia exhibits late summer/early autumn maxima at the two westernmost subarctic stations.

The average base run mean over all the midlatitude stations is 1.68 ng m^{-3}, which is the highest average of all three station groups. At the midlatitude stations, base run means are mainly higher than observed means (Fig. 3j–q); as at little Fox Lake and Fort Chipewyan, the model is unable to reproduce the seasonal decrease in concentrations, typically observed in late summer/early autumn. A similar minimum was documented by Weiss-Penzias et al. (2007) at Mount Bachelor Observatory, Oregon. The cause of this minimum is an active area of research. The current working hypothesis is that it is produced by chemical activity and not by changes in the emissions. Short-term variability at these stations is captured remarkably well by the model. The observed mean for the midlatitude stations is 1.60 ng m^{-3}; the model's inability to capture the summer/autumn minimum leads to an overestimation of the station group average.

Asian concentrations range at the midlatitude stations from 0.5–0.7 ng m^{-3}. This is higher than values seen at arctic stations and comparable to those at subarctic stations. Asian concentrations exhibit a distinct late spring/early summer maximum at the three westernmost stations and, in late summer/early fall, at St. Anicet. North American concentrations are significantly higher than at the more northerly stations, with values often at 0.4 ng m^{-3} and frequently surpassing 0.6 ng m^{-3}. The great degree of variability in the North American concentrations indicates the close proximity of a local source. At Burnt Island, Egbert, and St. Anicet, the variabilities in the North American, base run and observed concentrations follow each other closely; it is a much easier task for the

CC BY

model to reproduce observed values when an important local source, well-represented in the emissions, dominates the behaviour of the observations. Russian and European concentrations are comparable to those at the subarctic stations. Russian concentrations exhibit a late summer/early autumn maximum, which is most noticeable in the westernmost stations. The onset of the Russian maximum starts earlier as one moves westwards and northwards.

Concerning model verification, we are able to state that, at a first level, the base model run was able to reproduce observed ambient GEM concentrations fairly well at each of our stations. We conclude that meteorological and chemical processes are similar at these sites.

3.1.2 Percent contribution

Figure 4 indicates that the four source regions together contribute, on average, 56% of the base run's TGM/GEM concentrations. This significant elevation of the combined contribution over the 46% of total emissions produced by our four source regions (Fig. 2) reflects the fact that Northern Hemispheric emissions are greater than those of the Southern Hemisphere, and suggests that interhemispheric mixing is suboptimal. The lowest total contributions (≈52%) are found in midlatitudes at 600 hPa in autumn and winter, while the consistently highest contributions (≈62%) are found from the surface up to 850 hPa, in the Arctic and subarctic during autumn; inter-hemispheric transport occurs most strongly at higher altitudes and lower latitudes and during autumn. (Note that we only consider levels up to 600 hPa, as Stohl (2006) demonstrated that only Asian air parcels up to 600 hPa eventually reached the Arctic lower troposphere during winter. The levels 925, 850 and 600 hPa are just above the boundary layer, in the lower free troposphere, and in the mid troposphere, respectively.) One might expect our highest total contributions at high latitudes to occur during winter, not autumn; only high latitude pollution sources are expected to penetrate the polar dome during the coldest periods (Stohl, 2006; Law and Stohl, 2007). However, mercury's long lifetime permits it to travel polewards from lower latitudes, where it can mix with

ACPD
10, 4673–4717, 2010

cold high-latitude air parcels over time before penetrating the polar dome. The stronger winds of winter (Fig. 7) are presumably able to transport the mercury more efficiently than during autumn, when the winds are weaker.

Asia contributes by far the greatest portion of atmospheric gaseous mercury (29–37%) at all stations, seasons and levels considered. This is not unexpected, given that Asian emissions represent 30% of the total (Fig. 2). This Asian contribution corresponds well with previous estimates in the literature: Strode et al. (2008) show Asian surface-level mercury contributions over North America ranging from 31–36%; Travnikov (2005) calculated that 33% of Arctic mercury deposition originated in Asia; since there are no local sources, deposition is proportional to the percent contribution of atmospheric mercury. Unexpectedly, our Asian contribution does not decrease from summer to winter at arctic stations; mercury's long lifetime is likely counteracting the traditional difficulty that pollution from warm source regions encounters when attempting to penetrate high latitudes in winter (Stohl, 2006; Law and Stohl, 2007).

Strode et al. (2008) calculated a surface-level contribution from North American sources, averaged over the entire U.S.A, of 20%. The eight Canadian midlatitude stations are characterized by an average of 14%; our lower average reflects the fact that there are more mercury emissions is the USA than in Canada (Fig. 2).

Our European percent contributions range between 4.5% and 7.5%, with the higher values in the Arctic. Except at Andoya, for which Europe is a local source, contributions decrease only minimally with height. This contradicts the statement by Stohl et al. (2002) that, because of less vigorous convection and less frequent cyclogenesis, European emissions tend to remain in the lower troposphere. This apparent contradiction is possibly resolved by the long lifetime of mercury; their simulation, which did not involve mercury, lasted only one year, while we find a spinup period of at least three years necessary to reach a balanced global distribution of mercury. Our results also disagree with Travnikov (2005), who estimated that Europe contributes 22% of the mercury deposition in the Arctic. Given the distance between European emissions and the Arctic, this result suggests that Europe also contributed 22% of the ambient

mercury. This discrepancy is likely a result of differences in the emission fields used. Travnikov (2005) used anthropogenic emissions from 1995, where the European contribution is estimated at 250 tonnes by Pacyna et al. (2003). We used emissions from either 2000 or 2005. By 2000, European emissions were estimated to have dropped by some 30% to 175 tonnes (Pacyna et al., 2006).

Eleftheriadis et al. (2009) determined that black carbon concentrations at Ny-Ålesund originated mainly in Russia. This disagrees with our finding that Russia contributes only a small percentage of the ambient mercury at Ny-Ålesund. The difference in lifetimes is likely responsible for this discrepancy.

In general, the Asian contribution increases with altitude in all seasons at all stations. This behaviour, which is the signature of a non-local mercury source, is most pronounced at midlatitude stations, where North America is a local source. Conversely, the signature of a local source is the decrease with altitude of the source region's contribution. North America is a local source at all subarctic and midlatitude stations in all seasons. The importance of North America as a local source diminishes rapidly with latitude. Thus, the noticeable Asian increase in percent contribution with elevation at the midlatitude stations is simply a consequence of the strength of North America as a local source at these stations. Russia is a local source at Amderma, and Europe at Andoya.

3.1.3 Correlation squared

Concentrations from all source regions are highly correlated in spring with the base run's surface-level concentrations at subarctic Kuujjuarapik and at all arctic stations, except at Andoya. This reflects the dominance of AMDE dynamics in determining the variability at these stations during this season (Fig. 5). At Andoya, the competition between the weak AMDEs (Berg et al., 2008) and the strong transport from Europe (Fig. 3) to determine the base run's variability explains the reduced springtime surface-level correlations for all source regions' concentrations.

In all other situations, Asia tends to dominate the base run's variability. Asian corre-

ACPD
10, 4673–4717, 2010

lations are frequently valued near unity at all levels. This suggests either that mercury from Asia moves in a deep wave through the atmosphere, or that, regardless of the transport level, Asian mercury plumes are characterized by sufficiently high mercury concentrations that they are able to dominate individually the base run's variability. Both behaviours have been documented in the literature: Jaffe et al. (2005) noted the coherence with altitude of an air mass causing an Asian LRT event in Oregon; Radke et al. (2007) observed Asian mercury being transported in individual mercury-rich layers. The strong Asian correlations in the Arctic break down in winter, when it is most difficult for mercury from this warm-temperature source to penetrate the polar dome (Stohl, 2006; Law and Stohl, 2007). At both arctic and subarctic stations, Asian correlations tend to decrease as one moves eastwards, presumably as a result of increased mixing of air parcels. At midlatitude stations, Asian correlations exhibit a distinctive wave pattern, which is mirrored by North American correlations. This pattern is generated by the behaviour of North American, not Asian, mercury: near a local source, variability in the base run is dominated by North America, which reduces the Asian influence. Away from these sources, the North American influence wanes, and Asia returns to its typically dominant behaviour. The similar correlations calculated for Burnt Island and Egbert are to be expected, given the strong correlation found between the mercury concentrations of these two stations by Kim et al. (2005).

Strode et al. (2008) calculated that Asian mercury explains 42% of the springtime variability and 57% of the annual variability at Mount Bachelor Observatory, Oregon. At Reifel Island, which is geographically our closest station, Asian mercury explains 65% and 69% of the surface-level variability in spring and summer, respectively, and 19% and 3% of the surface-level variability in autumn and winter, respectively. This contrary behaviour is likely explained by differences in the two sites' locations: Reifel Island is at sea level right next to the ocean and near Vancouver, while Mount Bachelor Observatory is 180 km inland at an altitude of 2.7 km, and mostly experiences free tropospheric air (Jaffe et al., 2005). Reduced Asian correlations indicate the dominance of a local source at Reifel Island in autumn and winter, and at Mount Bachelor in spring.

Weiss-Penzias et al. (2006, 2007) documented springtime transport events at Mount Bachelor Observatory that were attributed to local mercury sources.

3.1.4 Transport efficiency

Although, on average, Asia contributes the most mercury and explains most of the base run's variability at all 17 stations, Asia's transport efficiency is almost always less than that of North America and often less than that of Russia (Fig. 6), particularly during summer and autumn. Given that Asian and North American emissions are at comparable latitudes, the lower Asian efficiencies at the arctic stations might be considered somewhat surprising. Similarly, given that Russian emission sources are farther from the midlatitude stations than are the Asian sources, it appears to be somewhat surprising that Russian and Asian transport efficiencies are comparable at these stations. The difference is likely explained by Fig. 8, which demonstrates that the maximum concentrations due to Asian emissions tend to be located higher in the troposphere than those due to North American or Russian emissions; the greatest concentrations from Asian emissions, which would produce the strongest transport efficiencies, are often above our top level of 600 hPa. This supposition is supported by the tendency of Asian efficiencies to increase strongly with altitude. At subarctic and midlatitude stations, European efficiencies are always smaller than Asian efficiencies. In the Arctic, European efficiencies are smaller than Asian efficiencies most often in summer and autumn and least often in winter and spring.

The importance of Russian efficiencies in the Arctic in all seasons, and its dominance in summer and autumn, is to be expected, given that it is relatively close to the Arctic and is a high latitude source, so that its mercury is more easily able to penetrate the polar dome (Stohl, 2006; Law and Stohl, 2007). This Russian importance is supported by Stohl (2006). However, the lesser importance of our European transport efficiencies in the Arctic do not agree with most published results. During his study on aerosols, Stohl (2006), who calculated efficiencies for air parcels at or below 500 m that have resided 5 days or more north of 70° N during winter, placed European effi-

ACPD
10, 4673–4717, 2010

ciencies second to Russian efficiencies, followed by North America and Asia. Shindell et al. (2008), who did not have a Russian source region, found the same surface-level wintertime efficiency rankings as Stohl (2006) otherwise for a carbon monoxide-like tracer. Considering only wintertime surface-level transport efficiencies at Alert, Station Nord and Ny-Ålesund, which are well north of 70° N, we agree that Russia dominates, but rank North America unexpectedly second, and Europe on the same order of importance as Asia. The reason for this disagreement is likely the long lifetime of mercury. Stohl (2006) used back trajectories of no more than 30 days, while the tracers of Shindell et al. (2008) had a 50-day lifetime. It is not unreasonable to think that mercury that ends up at the surface in the Arctic after being transported for six month to two years may well originate in different regions than particles that have travelled for a fraction of that time. In fact, some sensitivities calculated by Stohl (2006) yielded minimal differences between Europe and North America. Furthermore, Lin et al. (2001) found that Europe was a less important source of mercury for Alert during winter than Russia or North America. Lin et al. (2001) also found evidence that, even during winter, Asian mercury was reaching Alert.

In the Arctic, Russian efficiencies often maximize at 850 hPa. However, Russian efficiencies at Amderma and, to a lesser extent, at Andoya, tend to decrease with altitude. This tendency to decrease with altitude is also observed at all arctic stations during winter. Similarly, European wintertime transport efficiencies for the Arctic tend to be smallest at 600 hPa, particularly at nearby Ny-Ålesund, Andoya and Amderma. This agrees with findings from Stohl (2006) and Shindell et al. (2008). Our wintertime Asian efficiencies in the Arctic tend to increase with altitude, but often only minimally. Stohl (2006) and Shindell et al. (2008) both found an increase with altitude. The tendency for our North American transport efficiencies at arctic stations to increase with altitude during autumn and winter is also confirmed by Shindell et al. (2008).

North American efficiencies tend to dominate at subarctic stations and dominate overwhelmingly at midlatitude stations. This is to be expected, given the proximity to emission sources.

ACPD
10, 4673–4717, 2010

3.1.5 LRT events

The six arctic stations together recorded 470 LRT events per year, averaging 78 events per station (Table 2). The three subarctic stations also averaged 78 events per station per year, recording 234 events in all. 442 events per year were recorded between the eight midlatitude stations, yielding an average of 55 events per station. The distribution of events within a station group is discussed below.

Asia was responsible for the majority of all LRT events, producing 43%, 67% and 75% of the events at the arctic, subarctic and midlatitude stations, respectively. LRT events are only defined for North America at arctic stations (see Sect. 2.3.2). At these stations, North America contributed 16% of all events. The greatest share of Russian LRT events was at subarctic stations (33%), followed by arctic (27%) then midlatitude stations (23%). Europe's LRT events occurred almost exclusively in the Arctic (14%), with none at any subarctic station, and only 2% at midlatitude stations.

In the Arctic, Asian and North American LRT events occurred preferentially in summer, while both Russian and European events occurred preferentially in winter (Fig. 3, Table 2). Stohl (2006) found that the mean Arctic age of air increased from January to July at all our verification stations. This would lead us to expect fewer LRT events in summer than winter; the Asian and North American behaviour is unexpected. However, our verification stations are located in high gradient areas of the mean Arctic age of air fields calculated by Stohl (2006); these areas may be less accurate. Moreover, the overall age of air was found to be shorter in January on the European/Russian side of the Arctic than on the North American side, indicating that European and Russian air masses penetrate nearby Arctic regions in wintertime more easily than Asian or North American air masses. This agrees with our Russian/European winter LRT preference versus our Asian/North American summer preference. Lin et al.'s (2001) lack of evidence of summertime mercury LRT events at Alert may be an artifact of their 10-day back trajectories; weak summer winds transport air masses slowly. The fewest arctic events occur in spring for all source regions, presumably because local AMDE

ACPD
10, 4673–4717, 2010

dynamics mask the less vigorous variations in model concentrations caused by LRT events. This masking of springtime mercury LRT events by AMDEs is confirmed by Lin et al. (2001). In contrast, Warneke et al. (2009) found spring to be an active LRT season in the Arctic for aerosols, which do not participate in AMDEs, finding 50 plumes during six flights in the vicinity of Barrow. Biomass burning in Russia was identified as the source of these plumes.

Subarctic LRT events, which are produced only by Asia and Russia, occur most often in autumn, and least often in spring. The masking effect of Kuujjuarapik's AMDEs will have lowered the spring LRT count for this entire station group. In the midlatitude stations, where there are no AMDEs, Russia was most active in summer, but both Asia and Europe generated their greatest number of events in spring. This springtime preference for the trans-Pacific transport of Asian pollution was confirmed by Wang et al. (2009) and Liang et al. (2004).

Considering individual stations, Asia generates the most LRT events at the three lower latitude arctic stations (Barrow, Amderma and Ny-Ålesund) and at the two westernmost stations of the midlatitude group (Fig. 3, Table 3). Reifel Island's unexpectedly low number of Asian LRT events is possibly due to its sea-level elevation. Asian carbon monoxide LRT events are known to reach eastern North America, despite the effects of mixing and dilution (Ding et al., 2009). However, our high frequency of Asian LRT events at east coast Mingan is surprising. North American LRT events occurred most and least frequently at Barrow and Alert, respectively. This distribution is fully explained by Fig. 7, which will be discussed in Sect. 3.2.1. Alert, on the other hand, received the most Russian LRT events of any arctic station. At subarctic and midlatitude stations, Russian LRT events occurred preferentially at western stations. The occurrence of Russian LRT events in northwestern North America is also documented by Bertschi and Jaffe (2005). Not surprisingly, European LRT events are more frequent at nearby Amderma and Ny-Ålesund than the other arctic stations. On the other hand, the fact that midlatitude Kejimkujik and Mingan both experience European LRT events is unexpected. These events will also be explained in Sect. 3.2.1.

ACPD
10, 4673–4717, 2010

Comparing the LRT statistics at neighbouring arctic stations (Table 3), Ny-Ålesund and Amderma recorded almost identical numbers of events, despite the distance separating them. This suggests that they are governed by similar dynamics and transport pathways. Similarly, Station Nord, which is far closer to Ny-Ålesund than Amderma, experienced similar numbers of LRT events as Ny-Ålesund from Asia, North America and Russia. However, the number of recorded European events at these two stations differs significantly. Alert is no farther from Station Nord than Ny-Ålesund. However, while Alert recorded a comparable number of European events as Station Nord, it recorded almost twice as many Russian events and just over half as many North American events; the dynamics governing mercury concentrations at these two stations are very different. Alert also behaves very differently than Barrow. Similarly, Andoya and Ny-Ålesund, despite their proximity, behave quite differently. Thus, one cannot decide that dynamics and transport pathways affecting two separate locations will be similar or dissimilar based on proximity alone.

Interestingly, transport efficiencies and percent contributions do not always support the behaviour apparent in the LRT event statistics. For instance, Russian surface-level contributions and efficiencies at Alert and Station Nord are almost identical, despite the fact that Alert recorded nearly double the number of Russian LRT events. An LRT event consists of a high mercury concentration pulse, preceded and followed by lower concentration air masses; a direct route from the source to the station is required. In contrast, the efficiency and contribution are based on the amount of mercury that has reached a station over an entire season; indirect routes, involving considerable mixing, that deliver smaller amounts of mercury over longer periods are possible. Thus, there is no reason why the LRT statistics should be supported by the transport efficiencies and percent contributions; the types of transports are very different.

ACPD
10, 4673–4717, 2010

3.2 Two-dimensional fields

3.2.1 Horizontal distributions

Long range transport of Asian mercury towards North America is clearly evident in Fig. 7's column burden of GEM from the surface to 516 sigma (≈523 hPa, ≈5 km). Spring and autumn transports are mainly zonal, with the latter stronger than the former. Summer experiences the strongest trans-Pacific transport, with the greatest burden of mercury transported, over the widest latitudinal band, and with the strongest penetration into western North America and the Arctic; increased summertime emissions from land surfaces have more than compensated for weaker trans-Pacific winds. These results are supported by Jiang et al. (2007), who found that Asian carbon monoxide concentrations over the north Pacific were highest in summer, followed by autumn then spring. The preference for Asian springtime LRT events at the midlatitude stations (see Sect. 3.1.5) seems to contradict the stronger summertime trans-Pacific transport of Fig. 7. It is likely that more mixing occurs during summer, so that fewer high concentration pollution plumes reach North America. This supposition is supported by Fig. 8, which indicates that the vertical gradient of Asian concentrations over the Pacific Ocean is smallest in summer at all latitude bands; convection, which is strongest in summer over the region of maximum Asian mercury emissions (Jiang et al., 2007), has mixed the atmosphere. Asian mercury is transported to the Arctic during summer and autumn, and gradually dissipates during winter and spring.

The North American mercury burden up to 5 km is transported primarily to the North Atlantic Ocean, and from there east to Europe and north to the Arctic. Lesser amounts of mercury are transported to the equatorial Pacific and also from the south coast of Alaska directly towards Barrow. North American mercury is transported less vigorously to Alert. Thus, these average winds fully explain Table 3's maximum and minimum number of North American LRT events recorded at Barrow and Alert, respectively.

Europe's mercury is transported mainly zonally and polewards, with a strong penetration into the Arctic during autumn and winter; the polewards direction of this transport

produces the higher transport efficiencies at arctic stations during autumn and winter.

Most of the European LRT events recorded at arctic stations occurred during autumn and winter. During these seasons, Station Nord experiences average winds that have a westerly component. This component explains why Station Nord recorded so few European events compared to Ny-Ålesund, which receives a considerable amount of European mercury during both seasons.

It is not evident from these average winds precisely how the air masses responsible for the European LRT events recorded at the easternmost midlatitude stations travelled to these sites. With such a low event frequency, we cannot expect average wind fields to reveal the route. However, it seems most likely that the high mercury concentration plumes crossed the Atlantic, given the stations' locations on the east coast. Since the events occurred mainly in spring and winter, it is likely that the Azores High was unusually weak during those times; such an anomalous atmospheric circulation would help the plumes to cross the Atlantic.

Russia's Arctic atmospheric burden is greatest in summer and autumn, possibly because of the summertime enhancement of land surface emissions, followed by winter. The high summer and autumn burdens possibly explain these seasons' strong Russian transport efficiencies reported in Sect. 3.1.4. The prevalence of wintertime Russian LRT events in the Arctic is possibly caused by the stronger wintertime winds; any LRT events produced by the equally strong spring winds are masked by AMDE dynamics (see Sect. 3.1.5).

3.2.2 Vertical distributions

Asian, North American and Russian mercury concentrations tend to increase at all three latitude bands throughout the column during spring and summer and to dissipate through autumn and winter (Fig. 8). The spring/summer augmentation of values may be driven by increasing insolation, which, in turn, forces an increase in the natural land emissions and reemissions. Note that the zonal winds are at their weakest in each latitude band during summer. Europe's deviant behaviour with respect to this

CC BY

annual cycle may be caused by the fact that the model's annual non-anthropogenic emissions are smaller for Europe than any of the other three source regions, along with the fact that the model's European non-anthropogenic emissions are smaller than its anthropogenic emissions.

Maximum mercury concentrations for all source regions and all three latitude bands tend to be found in the mid troposphere when not directly over a source region. This seems to contradict the springtime GEM vertical profiles from the northeast Pacific that were measured by Radke et al. (2007). These profiles show small to strongly negative vertical gradients from the surface to 8 km. Their lack of a mid-tropospheric maximum is probably a consequence of oceanic emissions increasing low-altitude concentrations; our source regions only include ocean emissions in coastal regions. Our mid-tropospheric maxima suggest, as was found by Strode et al. (2008) that the trans-Pacific transport of Asian mercury occurs preferentially at that level, although the transport descends to the surface. Weiss-Penzias et al. (2006) concluded that the trans-Pacific transport of mercury is more efficient at higher than lower altitudes. Similar results were reported by Liang et al. (2004) and Wang et al. (2009), who studied carbon monoxide transport, although the former study found that the trans-Pacific transport no longer reaches the surface in summer. This disagreement may be a consequence of the reduced summertime lifetime of carbon monoxide reported by the authors.

Asian concentrations decrease, while European and Russian concentrations increase with latitude band. For North America, the high concentration regions are most extensive in the 50°–65° band.

4 Summary

The base model run was able to reproduce observed ambient GEM concentrations fairly well at each of our 17 verification stations in the Arctic and across Canada. This indicates that meteorological and chemical processes are similar at these locations.

Of our four source regions, we find that Asia is the dominant source of mercury at

ACPD
10, 4673–4717, 2010

all stations, in all seasons, at all levels considered. Despite its relatively low transport efficiencies, it is characterized by the greatest percent contributions and tends to determine most of the base run's variability. It generated the most LRT events. North America behaves as a local source at the subarctic and midlatitude stations, with a tendency to contribute more mercury at the surface than in the mid-troposphere, determine the base run's variability, and exhibit the largest surface-level transport efficiencies. Similarly, Europe is a local source at Andoya and Russia at Amderma.

Considering transport to the Arctic, we find that Russian transport efficiencies are important, as expected, particularly in summer and autumn. However, our European efficiencies are lower and Asian efficiencies higher than those found in the literature. This unexpected result is likely explained by fact that most studies of transport to the Arctic concern aerosols and carbon monoxide. The transport of these two pollutants favours closer sources since their lifetimes are far shorter than that of mercury.

The accepted springtime preference for the trans-Pacific transport of Asian pollution was evident only in the midlatitude group of stations, being masked in the arctic and subarctic groups by the occurrence of AMDEs. Although LRT events from specific source regions tended to be recorded preferentially in certain regions, for instance Russian events at the western stations of the subarctic and midlatitude groups, we determined that the dynamics and transport pathways affecting mercury concentrations at two separate arctic locations are not defined by proximity alone.

We find that the column burden of GEM in the lowest 5 km is largest in summer for Asia, North America and Russia, but in winter for Europe. In the vertical, transport of mercury from all source regions occurred principally in the mid-troposphere in all three latitude bands considered.

Acknowledgements. This research was funded by the International Polar Year (IPY) project, Intercontinental Atmospheric Transport of Anthropogenic Pollutants to the Arctic (INCATPA). We are grateful to all those who provided data. Henrik Skov is acknowledged for the GEM concentrations from Station Nord; the Danish Environmental Protection Agency financially supported his work with means from the MIKA/DANCEA funds for Environmental Support to the Arctic Region. We thank Hayley Hung, Alexandra Steffen, Pierrette Blanchard and the two anonymous

reviewers for their helpful comments.

References

Almeida, M. D., Lacerda, L. D., Bastos, W. R., and Herrmann, J. C.: Mercury loss from soils following conversion from forest to pasture in Rondonia, Western Amazon, Brazil, Environ. Pollut., 137, 179–186, 2005.

Berg, T., Aspmo, K., and Steinnes, E.: Transport of Hg from atmospheric mercury depletion events to the mainland of Norway and its possible influence on Hg deposition, Geophys. Res. Lett., 35, L09802, doi:10.1029/2008GL033586, 2008.

Bertschi, I. T. and Jaffe, D. A.: Long-range transport of ozone, carbon monoxide, and aerosols to the NE Pacific troposphere during the summer of 2003: Observations of smoke plumes from Asian boreal fires, J. Geophys. Res., 110, D05303, doi:10.1029/2004JD005135, 2005.

Côté, J., Desmarais, J.-G., Gravel, S., Méthot, A., Patoine, A., Roch, M., and Staniforth, A.: The operational CMC-MRB Global Environmental Multiscale (GEM) Model: Part II – Results, Mon. Weather Rev., 126, 1397–1418, 1998a.

Côté, J., Gravel, S., Méthot, A., Patoine, A., Roch, M., and Staniforth, A.: The operational CMC-MRB Global Environmental Multiscale (GEM) Model: Part I – Design considerations and formulation, Mon. Weather Rev., 126, 1373–1395, 1998b.

Dastoor, A. P., Davignon, D., Theys, N., Van Roozendael, M., Steffen, A., and Ariya, P. A.: Modeling dynamic exchange of gaseous elemental mercury at polar sunrise, Environ. Sci. Technol., 42, 5183–5188, 2008.

Dastoor, A. P. and Larocque, Y.: Global circulation of atmospheric mercury: a modelling study, Atmos. Environ., 38, 147–161, 2004.

Ding, A., Wang, T., Xue, L., Gao, J., Stohl, A., Lei, H., Jin, D., Ren, Y., Wang, X., Wei, X., Qui, Y., Liu, J., and Zhang, X.: Transport of north China air pollution by midlatitude cyclones: Case study of aircraft measurements in summer 2007, J. Geophys. Res., 114, D11399, doi:10.1029/2009JD012339, 2009.

Eleftheriadis, K., Vratolis, S., and Nyeki, S.: Aerosol black carbon in the European Arctic: Measurements at Zeppelin station, Ny-Ålesund, Svalbard from 1998–2007, Geophys. Res. Lett., 36, L02809, doi:10.1029/2008GL035741, 2009.

Faïn, X., Obrist, D., Hallar, A. G., Mccubbin, I., and Rahn, T.: High levels of reactive gaseous

mercury observed at a high elevation research laboratory in the Rocky Mountains, Atmos. Chem. Phys., 9, 8049–8060, 2009, http://www.atmos-chem-phys.net/9/8049/2009/.
Fitzgerald, W. F., Engstrom, D. R., Lamborg, C. H., Tseng, C.-M., Balcom, P. H., and Hammerschmidt, C. R.: Modern and historic atmospheric mercury fluxes in northern Alaska: Global sources and Arctic depletion, Environ. Sci. Technol., 39, 557–568, 2005.
Fouquart, Y. and Bonnel, B.: Computations of solar heating of the earth's atmosphere: a new parameterization, Contrib. Atmos. Phys., 53, 35–62, 1980.
Garand, L. and Mailhot, J.: The influence of infrared radiation on numerical weather forecasts, in: Proceedings of the Seventh Conference on Atmospheric Radiation, San Francisco, USA, 23–27 July 1990, J146–J151, 1990.
Gbor, P. K., Wen, D., Meng, F., Yang, F., and Sloan, J. J.: Modeling of mercury emission, transport and deposition in North America, Atmos. Environ., 41, 1135–1149, 2007.
Goulet, R. R., Holmes, J., Page, B., Poissant, L., Siciliano, S. D., Lean, D. R. S., Wang, F., Amyot, M., and Tessier, A.: Mercury transformations and fluxes in sediments of a riverine wetland, Geochim. Cosmochim. Ac., 71, 3393–3406, 2007.
Jaffe, D., Prestbo, E., Swartzendruber, P., Weiss-Penzias, P., Kato, S., Takami, A., Hatakeyama, S., and Kajii, Y.: Export of atmospheric mercury from Asia, Atmos. Environ., 39, 3029–3038, 2005.
Jiang, J. H., Livesey, N. J., Su, H., Neary, L., McConnell, J. C., Richards, N. A. D.: Connecting surface emissions, convective uplifting, and long-range transport of carbon monoxide in the upper troposphere: New observations from the Aura Microwave Limb Sounder, Geophys. Res. Lett., 34, L18812, doi:10.1029/2007GL030638, 2007.
Kim, K.-H., Ebinghaus, R., Schroeder, W. H., Blanchard, P., Kock, H. H., Steffen, A., Froude, F. A., Kim, M.-Y., Hong, S., and Kim, J.-H.: Atmospheric mercury concentrations from several observatory sites in the Northern Hemisphere, J. Atmos. Chem., 50, 1–24, 2005.
Law, K. S. and Stohl, A.: Arctic air pollution: origins and impacts, Science, 315, 1537–1540, 2007.
Lehrer, E., Hönninger, G., and Platt, U.: A one dimensional model study of the mechanism of halogen liberation and vertical transport in the polar troposphere, Atmos. Chem. Phys., 4, 2427–2440, 2004, http://www.atmos-chem-phys.net/4/2427/2004/.
Liang, Q., Jaeglé, L., Jaffe, D. A., Weiss-Penzias, P., Heckman, A., and Snow, J. A.: Long-

range transport of Asian pollution to the northeast Pacific: Seasonal variations and transport pathways of carbon monoxide, J. Geophys. Res., 109, D23S07, doi:10.1029/2003JD004402, 2004.

Lin, C.-J., Cheng, M.-D., and Schroeder, W. H.: Transport patterns and potential sources of total gaseous mercury measured in Canadian high Arctic in 1995, Atmos. Environ., 35, 1141–1154, 2001.

Lin, C.-J., Pongprueksa, P., Lindberg, S. E., Pehkonen, S. O., Byun, D., and Jang, C.: Scientific uncertainties in atmospheric mercury models I: Model science evaluation, Atmos. Environ., 40, 2911–2928, 2006.

Lohman, K., Seigneur, C., Gustin, M., and Lindberg, S.: Sensitivity of the global atmospheric cycle of mercury to emissions, Appl. Geochem., 23, 454–466, 2008.

Mason, R.: Mercury emissions from natural processes and their importance in the global mercury cycle, Mercury fate and transport in the global atmosphere, Springer US, 173–191, 2009.

Mitchell, C. P. J., Branfireun, B. A., and Kolka, R. K.: Assessing sulfate and carbon controls on net methylmercury production in peatlands: An in situ mesocosm approach, Appl. Geochem., 23, 503–518, 2008.

Pacyna, E. G., Pacyna, J. M. Steenhuisen, F., and Wilson, S.: Global anthropogenic mercury emission inventory for 2000, Atmos. Environ., 40, 4048–4063, 2006.

Pacyna, J. M., Pacyna, E. G., Steenhuisen, F., and Wilson, S.: Mapping 1995 global anthropogenic emissions of mercury, Atmos. Environ., 37, 109–117, 2003.

Radke, L. F., Friedli, H. R., and Heikes, B. G.: Atmospheric mercury over the NE Pacific during spring 2002: Gradients, residence time, upper troposphere lower stratosphere loss, and long-range transport, J. Geophys. Res., 112, D19305, doi:10.1029/2005JD005828, 2007.

Ryaboshapko, A., Bullock, O. R. Jr., Christensen, J., Cohen, M., Dastoor, A., Ilyin, I., Petersen, G., Syrakov, D., Artz, R., Davignon, D., Draxler, R. R., and Munthe, J.: Intercomparison study of atmospheric mercury models: 1. Comparison of models with short-term measurements, Sci. Total Environ., 376, 228–240, 2007a.

Ryaboshapko, A., Bullock, O. R. Jr., Christensen, J., Cohen, M., Dastoor, A., Ilyin, I., Petersen, G., Syrakov, D., Travnikov, O., Artz, R., Davignon, D., Draxler, R. R., Munthe, J., and Pacyna, J.: Intercomparison study of atmospheric mercury models: 2. Modelling results vs. long-term observations and comparison of country deposition budgets, Sci. Total Environ., 377, 319–333, 2007b.

Schroeder, W. H. and Munthe, J.: Atmospheric mercury – an overview, Atmos. Environ., 32, 809–822, 1998.
Shetty, S. K., Lin C.-J., Streets D. G., and Jang C.: Model estimate of mercury emission from natural sources in East Asia, Atmos. Environ., 42, 8674–8685, 2008.
Shindell, D. T., Chin, M., Dentener, F., Doherty, R. M., Faluvegi, G., Fiore, A. M., Hess, P., Koch, D. M., MacKenzie, I. A., Sanderson, M. G., Schultz, M. G., Schulz, M., Stevenson, D. S., Teich, H., Textor, C., Wild, O., Bergmann, D. J., Bey, I., Bian, H., Cuvelier, C., Duncan, B. N., Folberth, G., Horowitz, L. W., Jonson, J., Kaminski, J. W., Marmer, E., Park, R., Pringle, K. J., Schroeder, S., Szopa, S., Takemura, T., Zeng, G., Keating, T. J., and Zuber, A.: A multi-model assessment of pollution transport to the Arctic, Atmos. Chem. Phys., 8, 5353–5372, 2008,
http://www.atmos-chem-phys.net/8/5353/2008/.
Steen, A. O., Berg, T., Dastoor, A. P., Durnford, D. A., Hole, L. R., and Pfaffhuber, K. A.: Dynamic exchange of gaseous elemental mercury during polar night and day, Atmos. Environ., 43, 5604–5610, 2009.
Steffen, A., Schroeder, W., Macdonald, R., Poissant, L., and Konoplev, A.: Mercury in the Arctic atmosphere: An analysis of eight years of measurements of GEM at Alert (Canada) and a comparison with observations at Amderma (Russia) and Kuujjuarapik (Canada), Sci. Total Environ., 342, 185–198, 2005.
Stohl, A.: Characteristics of atmospheric transport into the Arctic troposphere, J. Geophys. Res., 111, D11306, doi:10.1029/2005JD006888, 2006.
Stohl, A., Eckhardt, S., Forster, C., James, P., and Spichtinger, N.: On the pathways and timescales of intercontinental air pollution transport, J. Geophys. Res., 107, 4684, doi:10.1029/2001JD001396, 2002.
Strode, S. A., Jaeglé, L., Jaffe, D. A., Swartzendruber, P. C., Selin, N. E., Holmes, C., and Yantosca, R. M.: Trans-Pacific transport of mercury, J. Geophys. Res., 113, D15305, doi:10.1029/2007JD009428, 2008.
Sunderland, E. M., Krabbenhoft, D. P., Moreau, J. W., Strode, S. A., and Landing, W. M.: Mercury sources, distribution, and bioavailability in the North Pacific Ocean: Insights from data and models, Global Biogeochem. Cy., 23, GB2010, doi:10.1029/2008GB003425, 2009.
Swartzendruber, P. C., Jaffe, D. A., and Finley, B.: Improved fluorescence peak integration in the Tekran 2537 for applications with sub-optimal sample loadings, Atmos. Environ., 43, 3648–3651, 2009.

Travnikov, O.: Contribution of the intercontinental atmospheric transport to mercury pollution in the Northern Hemisphere, Atmos. Environ., 39, 7541–7548, 2005.

Wang, K., Zhang, Y., Jang, C., Phillips, S., and Wang, B.: Modeling intercontinental air pollution transport over the trans-Pacific region in 2001 using the Community Multiscale Air Quality modeling system, J. Geophys. Res., 114, D04307, doi:10.1029/2008JD010807, 2009.

Warneke, C., Bahreini, R., Brioude, J., Brock, C. A., de Gouw, J. A., Fahey, D. W., Froyd, K. D., Holloway, J. S., Middlebrook, A., Miller, L., Montzka, S., Murphy, D. M., Peischl, J., Ryerson, T. B., Schwarz, J. P., Spackman, J. R., and Veres, P.: Biomass burning in Siberia and Kazakhstan as an important source for haze over the Alaskan Arctic in April 2008, Geophys. Res. Lett., 36, L02813, doi:10.1029/2008GL036194, 2009.

Weiss-Penzias, P., Jaffe, D. A., Swartzendruber, P., Dennison, J. B., Chand, D., Hafner, W., and Prestbo, E.: Observations of Asian air pollution in the free troposphere at Mount Bachelor Observatory during the spring of 2004, J. Geophys. Res., 111, D10304, doi:10.1029/2005JD006522, 2006.

Weiss-Penzias, P., Jaffe, D., Swartzendruber, P., Hafner, W., Chand, D., and Prestbo, E.: Quantifying Asian.and biomass burning sources of mercury using the Hg/CO ratio in pollution plumes observed at the Mount Bachelor Observatory, Atmos. Environ., 41, 4366–4379, 2007.

Zhang, L., Brook, J. R., and Vet, R.: A revised parameterization for gaseous dry deposition in air-quality models, Atmos. Chem. Phys., 3, 2067–2082, 2003, http://www.atmos-chem-phys.net/3/2067/2003/.

Zhang, L., Moran, M. D., and Brook, J. R.: A comparison of models to estimate in-canopy photosynthetically active radiation and their influence on canopy stomatal resistance, Atmos. Environ., 35, 4463–4470, 2001.

Table 1. Verification stations.

Station	Station identifier	Latitude (°N)	Longitude (°E)	Elevation (m)	Observed species	Verification year	Data source
				Arctic stations			
Barrow, U.S.A.	BRW	71.3	-156.8	9	GEM	2000	Steve Brooks, National Oceanic and Atmospheric Administration, U.S.A.
Alert, Canada	ALT	82.5	-62.3	210	GEM	2000	CAMNet, http://www.msc-smc.ec.gc.ca/natchem/index_e.html, Canada
Station Nord, Greenland	SND	81.6	-16.7	20	GEM	2001	Henrik Skov, National Environmental Research Institute, Denmark
Ny-Ålesund, Norway	NYA	78.9	11.9	474	GEM	2008	Katrine Aspmo, Pfaffhuber, Norwegian Institute for Air Research, Norway
Andoya, Norway	AND	69.0	16.0	380	GEM	2004	Torunn Berg, Norwegian Institute for Air Research, Norway
Amderma, Russia	AMD	69.8	61.7	41	GEM	2008	Alexandra Steffen, Environment Canada
				Sub-arctic stations			
Little Fox Lake	LFL	61.4	-135.6	1128	TGM	2008	Alexandra Steffen, Environment Canada
Fort Chipewyan	FCH	58.8	-111.1	232	TGM	2001	Canadian National Atmospheric Chemistry Database, http://www.msc-smc.ec.gc.ca/natchem/index_e.html, Canada
Kuujjuarapik	YGW	55.3	-77.7	14	TGM	2006	
				Midlatitude stations			
Reifel Island (or Delta)	RFL	49.1	-123.2	0	TGM	2000	
Esther	EST	51.7	-110.2	707	TGM	2000	
Bratt's lake	BRL	50.2	-104.7	587	TGM	2006	
Burnt Island	BNT	45.8	-83.0	75	TGM	2000	Canadian National Atmospheric Chemistry Database, http://www.msc-smc.ec.gc.ca/natchem/index_e.html, Canada
Egbert	EGB	44.2	-79.8	251	TGM	2000	
St. Anicet	WBZ	45.1	-74.3	49	TGM	2005	
Kejimkujik	KEJ	44.4	-65.2	127	TGM	2001	
Mingan	WBT	50.3	-64.2	11	TGM	2000	

ACPD
10, 4673–4717, 2010

Table 2. Distribution of LRT events by season.

Source region	Spring	Summer	Autumn	Winter	Total	% of total
			Arctic stations			
Asia	33	70	64	34	201	43%
North America	12	27	20	18	77	16%
Russia	26	35	26	39	126	27%
Europe	5	9	21	31	66	14%
All 4 regions	76	141	131	122	470	100%
			Sub-arctic stations			
Asia	34	37	48	38	157	33%
North America	N/A	N/A	N/A	N/A	N/A	N/A
Russia	13	17	32	15	77	16%
Europe	0	0	0	0	0	0%
All 4 regions	47	54	80	53	234	50%
			Midlatitude stations			
Asia	97	78	88	70	333	71%
North America	N/A	N/A	N/A	N/A	N/A	N/A
Russia	24	28	25	24	101	21%
Europe	5	1	0	2	8	2%
All 4 regions	126	107	113	96	442	94%

Table 3. Distribution of LRT events by station.

			Arctic stations					
Source region	Barrow	Alert	Station Nord	Ny-Ålesund	Andoya	Amderma		
Asia	40	32	30	38	23	38		
North America	25	6	10	10	14	12		
Russia	27	33	17	20	29	N/A		
Europe	1	6	7	25	N/A	27		
All 4 regions	93	77	64	93	66	77		
			Sub-arctic stations					
Source region	Little Fox Lake	Fort Chipewyan	Kuujjuarapik					
Asia	61	59	37					
North America	N/A	N/A	N/A					
Russia	33	23	21					
Europe	0	0	0					
All 4 regions	94	82	58					
			Midlatitude stations					
Source region	Reifel Island	Esther	Bratt's Lake	Burnt Island	Egbert	St. Anicet	Kejimkujik	Mingan
Asia	37	55	56	29	30	42	32	52
North America	N/A	N/A	N/A	N/A	N/A	N/A	N/A	N/A
Russia	16	23	19	9	13	8	5	8
Europe	0	0	0	0	0	1	4	3
All 4 regions	53	78	75	38	43	51	41	63

ACPD
10, 4673–4717, 2010

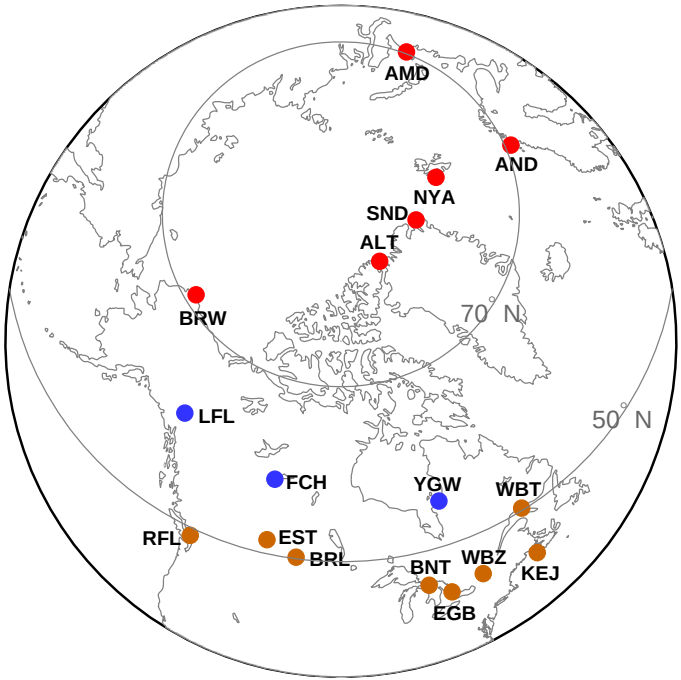

Fig. 1. Locations of verification stations. See Tables 1–3 for station names.

ACPD
10, 4673–4717, 2010

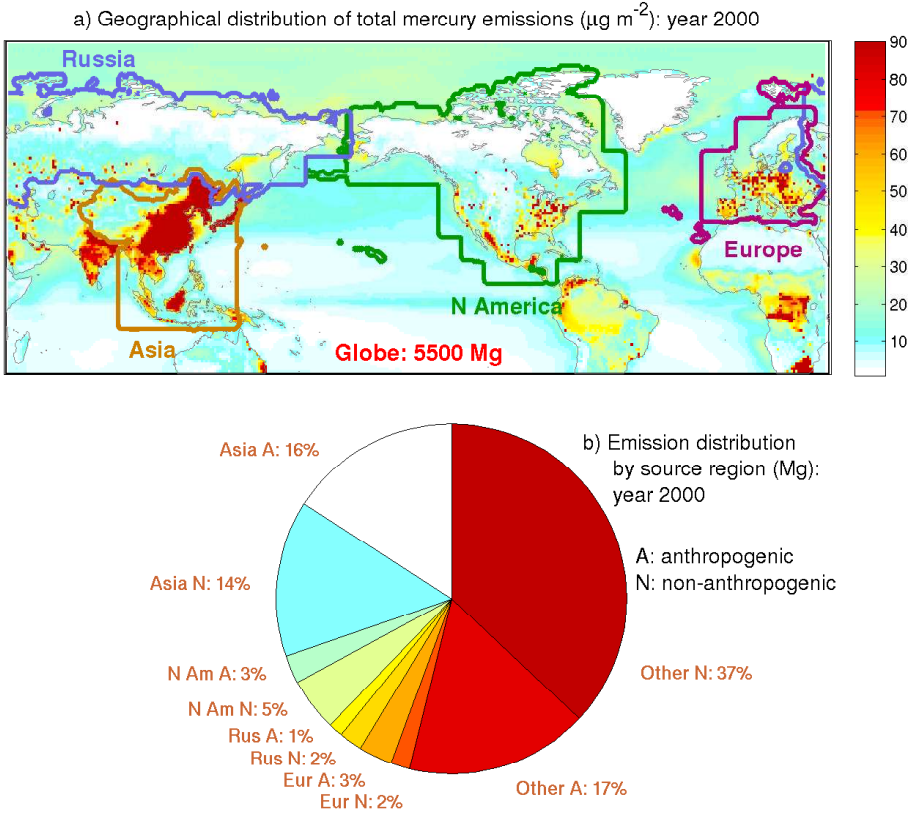

Fig. 2. Total mercury emissions for the study's four source regions and for the globe.

ACPD
10, 4673–4717, 2010

CC BY

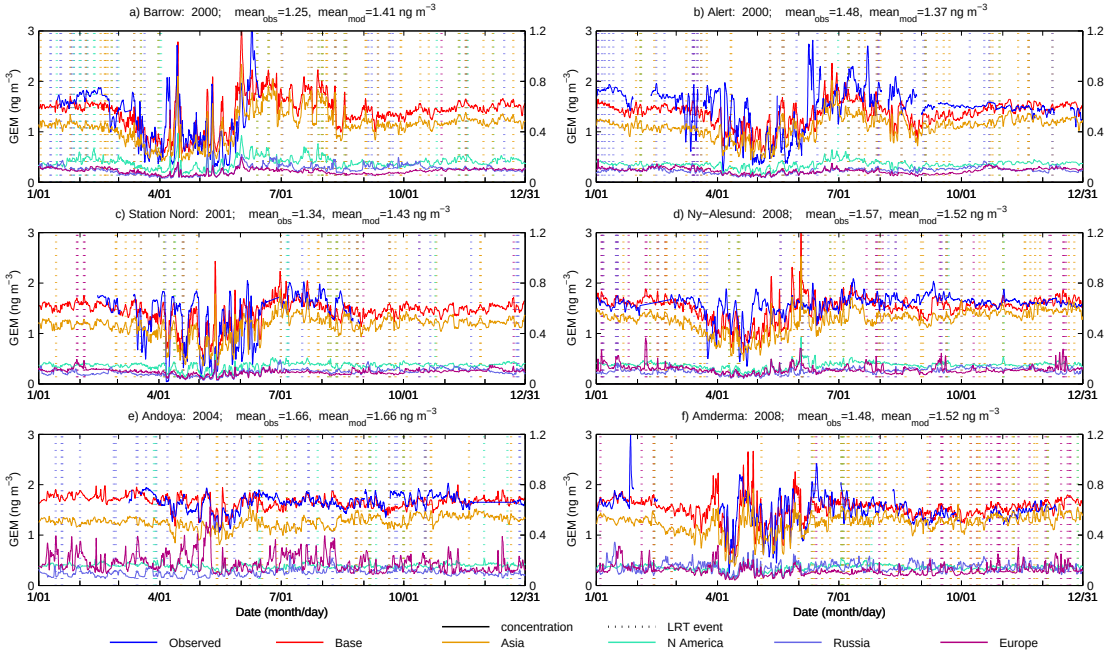

Fig. 3. Ambient surface-level GEM or TGM concentrations as observed at each verification station for the year indicated, and as simulated using emissions from the indicated source regions. The right hand axis pertains to observations and the base run. The left hand axis pertains to the simulations using emissions from only one of the four source regions. Note that axis limits are constant for panels **(a–f)** and **(j–q)**, but that those of panel **(i)** differ from those of panels **(g–h)**. Vertical dashed lines indicate LRT events. Stations from each station group are arranged from west to east.

ACPD
10, 4673–4717, 2010

CC BY

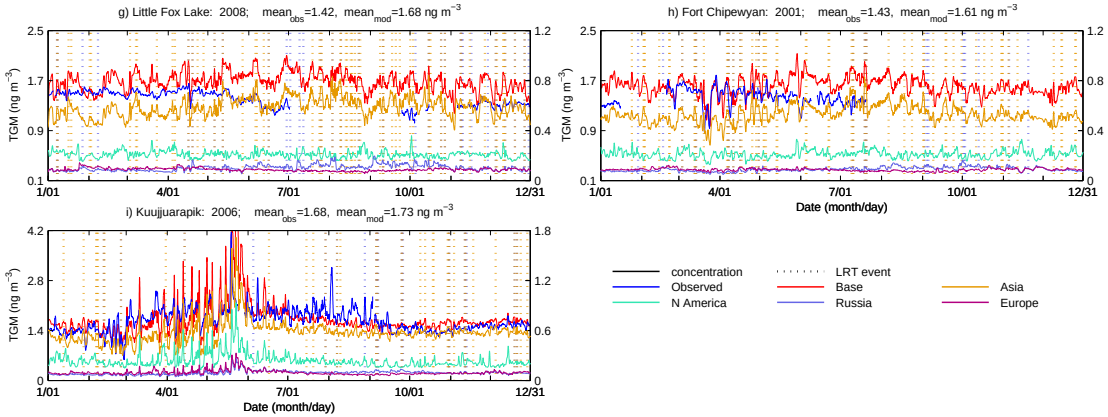

Fig. 3. Continued.

ACPD
10, 4673–4717, 2010

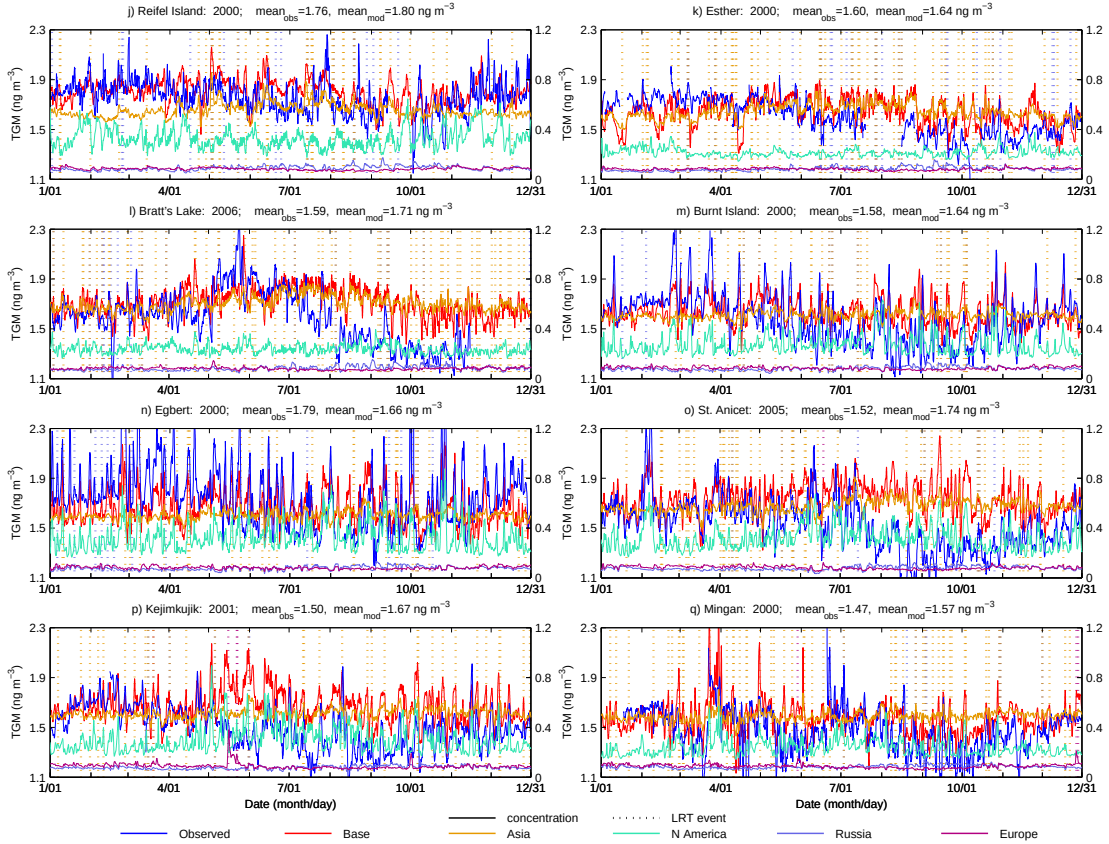

Fig. 3. Continued.

ACPD
10, 4673–4717, 2010

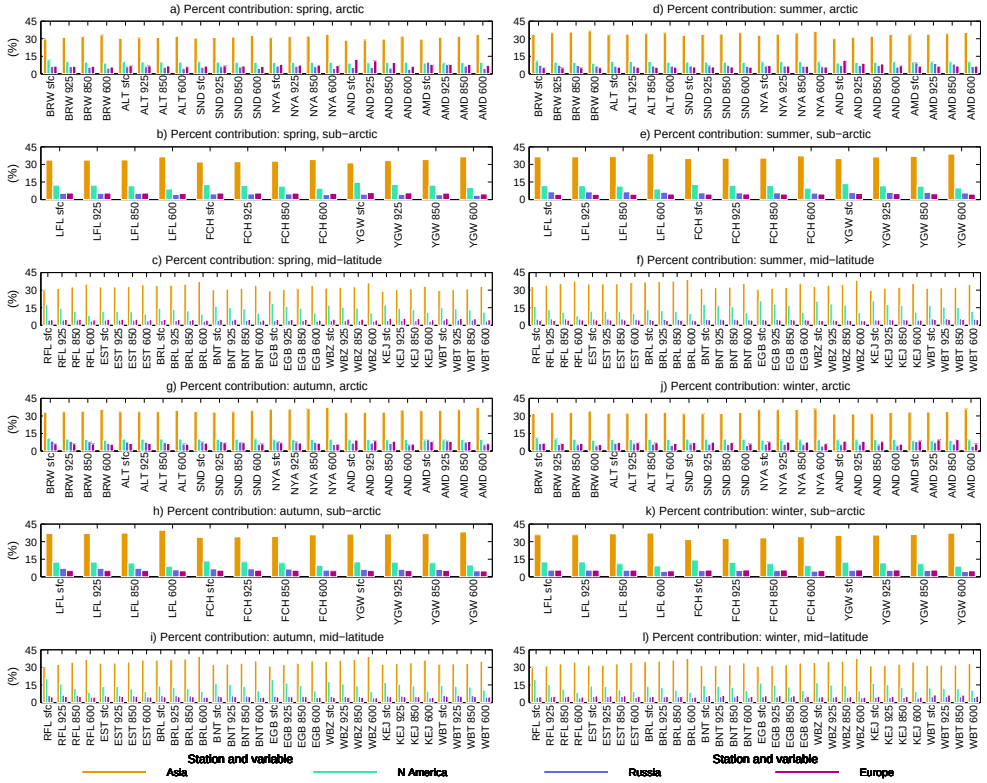

Fig. 4. Shown for the indicated station, level and season is each source region's percent contribution to the base run's concentrations. Table 1 identifies whether GEM or TGM contributions are calculated at the surface. GEM contributions are calculated at all stations at 925, 850 and 600 hPa. Stations from each station group are arranged from west to east.

ACPD
10, 4673–4717, 2010

CC BY

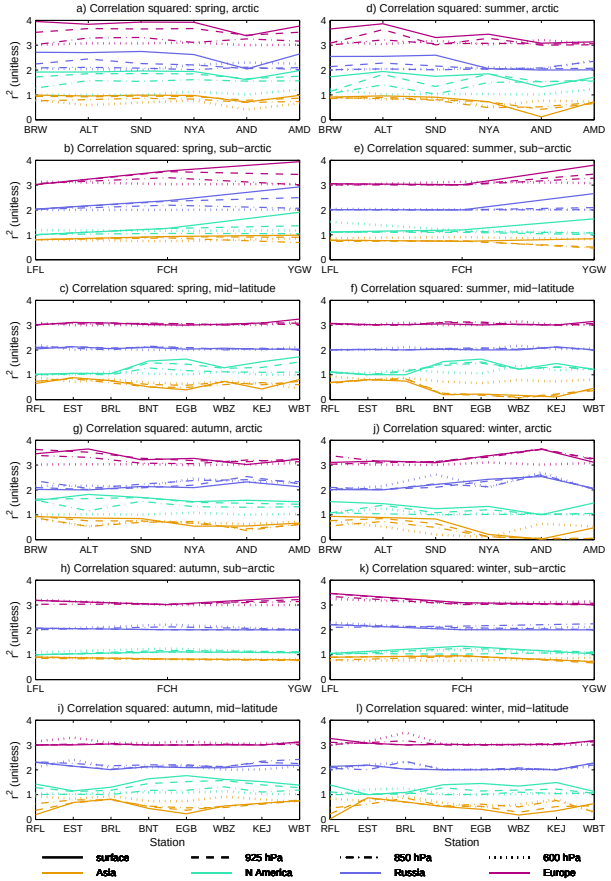

Fig. 5. Shown for each source region at the indicated station, level and season is the correlation squared between the base run's mercury concentrations and the concentrations simulated using the specified source region's emissions alone. Values from North America, Russia and Europe are increased successively by unity to promote readability. Table 1 identifies whether GEM or TGM correlations are calculated at the surface. GEM correlations are calculated at all stations at 925, 850 and 600 hPa. Stations from each station group are arranged from west to east.

ACPD
10, 4673–4717, 2010

CC BY

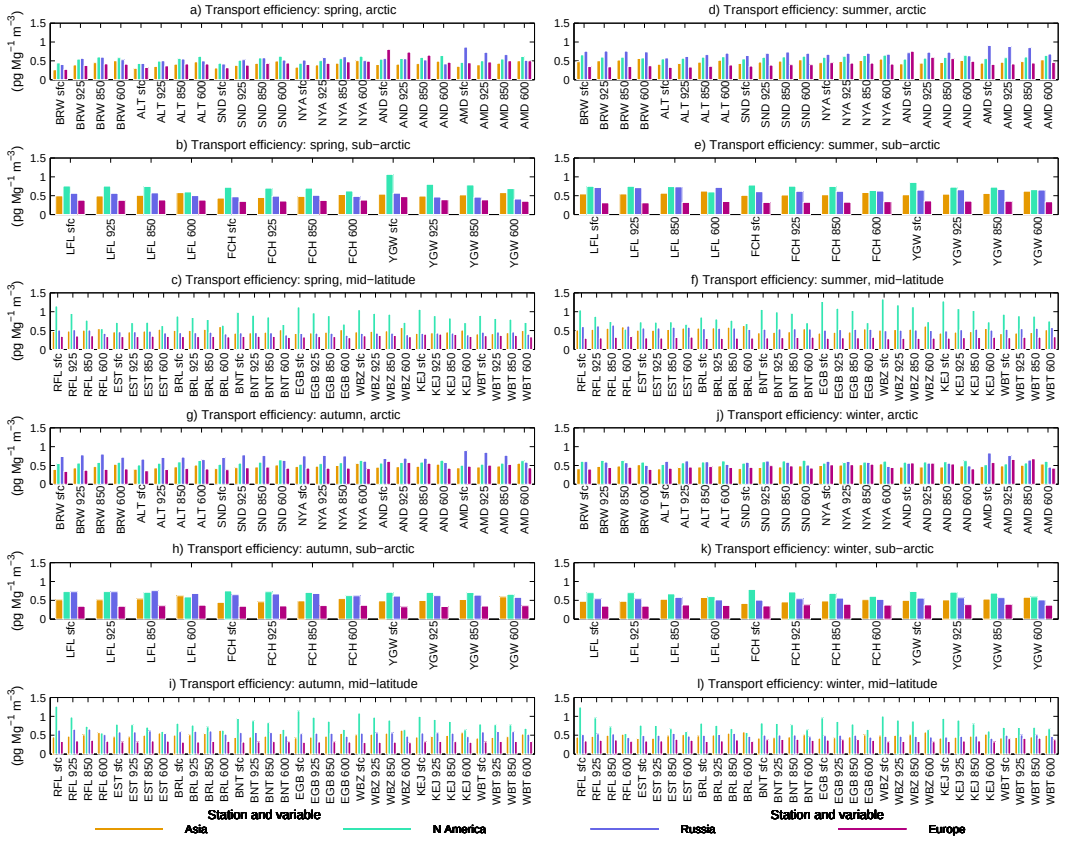

Fig. 6. Shown for the indicated station, level and season is each source region's transport efficiency. Table 1 identifies whether GEM or TGM efficiencies are calculated at the surface. GEM efficiencies are calculated at all stations at 925, 850 and 600 hPa. Stations from each station group are arranged from west to east.

ACPD
10, 4673–4717, 2010

CC BY

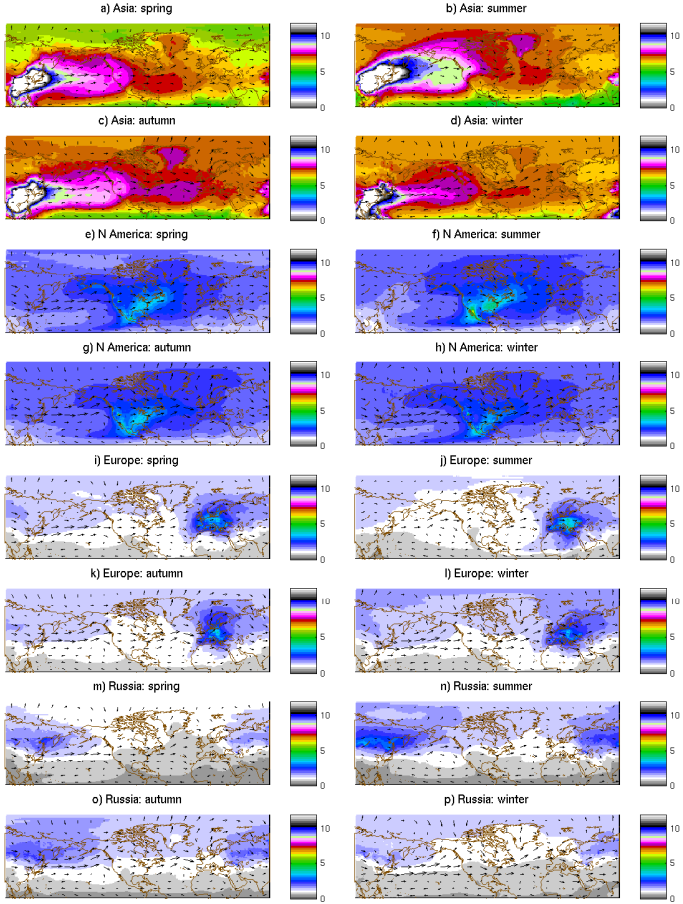

Fig. 7. Plotted for each source region and season for the year 2000 are: i) the GEM column burden (ng m^{-3}) from the surface to 516 sigma (≈523 hPa; shading interval of 0.3 ng m^{-3}), and ii) average wind directions and relative strengths calculated using winds from 925 to 400 hPa.

ACPD
10, 4673–4717, 2010

CC BY

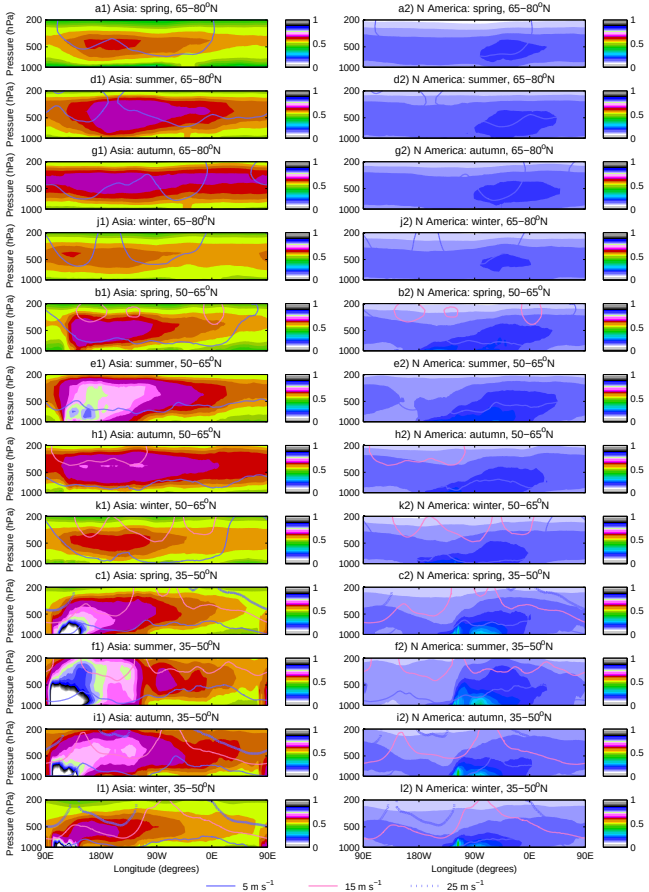

Fig. 8. Plotted for each source region and season for the year 2000 are vertical cross sections of: i) GEM (ng m^{-3}; shading interval of 0.025 ng m^{-3}), and ii) zonal wind strength. All values are averaged over the latitude band indicated.

ACPD
10, 4673–4717, 2010

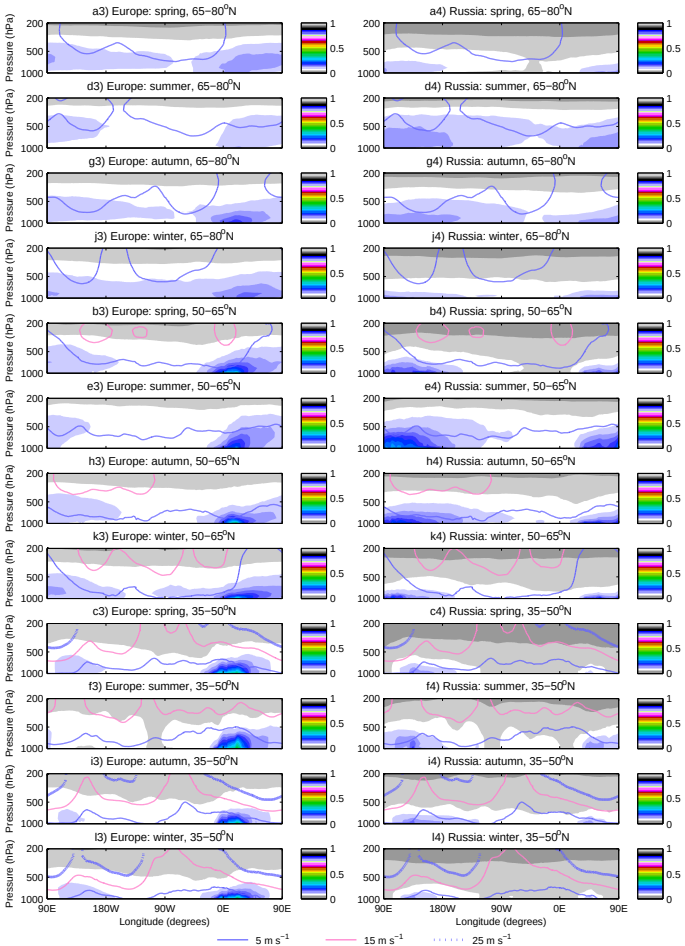

Fig. 8. Continued.

ACPD
10, 4673–4717, 2010